

The North Texas Convective Snow Event of 6 March 2008

Nicholas L. Hampshire
 Ted Ryan
National Weather Service, Fort Worth/Dallas, TX

1. Introduction

On 6 March 2008, a band of heavy snow developed across portions of North Texas and produced accumulations up to 30 cm (12 in). While snow occurred along a 145 km (90 mile) wide line from Northwest Texas to Northern Arkansas, the area of snowfall from Eastland County and Jack County (Texas) northeastward into Cooke County and Grayson County (Texas) will be the focus of study (Fig. 1). The snow began around 1700 UTC across Young, Jack, and Montague counties and persisted for two to four hours before shifting east. Snowfall rates in excess of 5 cm (2 in) per hour occurred with totals up to 30 cm (12 in) in Sherman, TX (Grayson County) (Fig. 2). A very sharp gradient of total snow accumulation occurred with this event. Denton, TX (Denton County) reported 18 cm (7 inches) of accumulation, while the Dallas Fort Worth (DFW) International Airport which is located 35 km (22 miles) SSE of Denton, TX, received only 2 cm (1.1 in). Ten miles further south and east of DFW only a trace of snow was observed across the city of Dallas.

Thunder was reported at several observation sites within the heavy snow band between 1800 and 1900 UTC. This snowfall event was an extraordinarily rare and intense event for North Texas, especially because it occurred in the month of March (Ryan and Hanes 2009).

The purpose of the study is to investigate the atmospheric conditions that led toward this heavy thundersnow event and to provide operational forecasters a better understanding of the complex interactions between dynamics, moisture, and instability when forecasting a winter precipitation event. This paper will identify the processes that were favorable for the formation and persistence of the heavy snow band, whether convection was slantwise or upright, and analyze the thermodynamic parameters that led to thundersnow.

2. Data and Methodology

Objective surface and upper air analyses completed by the Storm Prediction Center (SPC) and the Hydrometeorological Prediction Center (HPC) were used to determine the conditions of the atmosphere prior to the onset of the event. In addition, a thorough analysis of the radiosonde observations (RAOBs) from Fort Worth, TX (FWD) at 1200 UTC and 1800 UTC on 6 March was performed in this study. Output from the Rapid Update Cycle (RUC) model on a 40 km and 80 km grid was utilized as an hourly upper level analysis tool to calculate

Petterssen Frontogenesis, equivalent potential temperature (θ_e), equivalent potential geostrophic vorticity (EPV), and other pertinent fields. Radar data from the Weather Surveillance Radar-88 Doppler (WSR-88D) at Spinks Airport in Fort Worth, TX (KFWS) was used to analyze precipitation and convective trends. Snowfall accumulation data was compiled from COOP observers trained to measure snowfall, local airport observers, reports from local emergency officials, and reports from the public.

3. Synoptic Analyses

The surface data and upper air data from the 1200 UTC 6 March RAOBs across North America were analyzed. From this data, conditions in the atmosphere can be determined by looking at analyzed surface and upper air maps.

The surface analysis depicted a cold front south of North Texas extending from Central Louisiana to Houston, San Antonio, and into Northeastern Mexico (Fig. 3). A 1026 mb surface high was centered over Northern Kansas and was building southward behind the front. Surface temperatures at 1200 UTC over North Texas ranged from 3 to 6°C (upper 30s and lower 40s F) with dewpoints around negative 1°C (30°F). North winds at 10 to 15 knots and temperatures in southern Oklahoma of 0°C (32°F) implied cold air advection (CAA) was occurring over North Texas behind the cold front.

The 850 mb analysis showed a low developing over the Big Bend region of Texas, a trough over the Ohio Valley, and high pressure over the Rockies and Western US (Fig. 4). This synoptic pattern showed a deformation zone over North Texas extending northeast into Arkansas coincident with the 850 mb thermal gradient. Winds south of the 850 mb front were from the south at 20 to 25 knots with temperatures over South Texas ranging from 8°C to 12°C which indicates warm air advection (WAA) was occurring south of the 850 mb front.

The 700 mb analysis revealed a closed cyclonic circulation centered over eastern New Mexico and the 700 mb cold front extending from Southeast Missouri, into Central Oklahoma, and into the Texas Panhandle (Fig. 5). A warm front was analyzed south of the cold front and extended from Southern Arkansas and into North Texas. This warm front was most likely the remnants of a previous strong front which moved through the region three days prior to 6 March. Winds ahead of the 700 mb cold front were from the southwest at 25 to 30 knots, again implying that warm advection was occurring above the cold frontal layer.

The 500 mb analysis revealed a shortwave trough centered over central New Mexico, which was embedded within a deep and broad longwave trough over central North America (Fig. 6). This shortwave trough progressed eastward and provided large scale dynamic lift throughout the day over North Texas.

In summary, the surface cold front at 1200 UTC had pushed through North Texas, but the 700 mb front still remained north of the region. WAA was strong above the surface extending to about 700 mb and a shortwave trough to the west put North Texas in a favorable region for large scale ascent.

4. Mesoscale Analyses

The mesoscale environment above the surface will be analyzed through the use of the Rapid Update Cycle (RUC) model 0-hour forecast fields on a 40 km or 80 km grid. Real time data sources are assimilated into the model, including aircraft sounding data, in order to provide the best possible initial conditions and subsequent forecasts (Brusky and Mamrosh 2006). Aircraft sounding are derived from observations taken with instruments on commercial aircraft, and have been shown to be fairly accurate with respect to temperatures (Benjamin et al 1999). Because the Dallas-Fort Worth International Airport was within 40 km of the heavy snow band, it helped build confidence that the RUC 0-hour forecasts had a reasonably accurate thermal profile.

4.1 Assessing Frontogenesis

Frontogenesis is defined as the formation of a front or the intensification of an existing front's thermal gradient (Bluestein 1993). The theory of Frontogenesis has been well researched, and several processes, including horizontal wind deformation, have been correlated directly with the onset or intensification of frontogenesis (Bergeron 1928).

A deformation zone extending from north-central Texas into southeast Oklahoma and northern Arkansas at 1200 UTC 6 March was noted in the 850 mb analysis (see Fig. 4). RUC analyses showed the well defined deformation zone persisted through 1500 UTC in the 700 – 800 mb layer (Fig. 7). In accordance with the theory developed by Bergeron, RUC analyses between 1500 and 1800 UTC indicated that there was a rapid increase of frontogenesis values in the same region where deformation was present hours before. (Fig. 8).

Because frontogenesis creates an ageostrophic circulation to restore a thermal wind balance, upward adiabatic motions occur on the warm side of the front and downward motions occur on the cold side (Bluestein 1993). These upward motions induced by frontogenesis are significant, but are not solely responsible for the formation of precipitation. Other factors, including moisture and instability, need to be assessed when diagnosing the potential for heavy banded precipitation (Schultz and Schumacher 1999). The 500 to 1000 mb mean layer relative humidity

values at 1800 UTC were between 85 and 90 percent, and instability will be explored in the next section.

4.2 Assessing Instability

With any winter time convective event, the type of banding or convective potential and related heavy precipitation is dependent on instability type (Nicosia and Grumm 1998). The 1200 UTC FWD sounding depicts a stable inversion layer extending from 925 mb to 725 mb with steep lapse rates of 6.7 C km^{-1} up to 575 mb (Fig. 9). Once the frontogenesis at the 700 mb level commenced and adiabatic cooling eroded the stable inversion near 700 mb, air parcels forced upward via dynamic lifting quickly obtained their level of free convection. The 1800 UTC FWD sounding showed the impact of dynamic forcing and adiabatic lifting on the inversion at 725 mb as well as the role warm-moist advection between 750 and 800 mb played in contributing to instability (Fig. 10).

While using observation or forecast soundings can be an adequate method for assessing instability at specific points, equivalent potential vorticity (EPV) can be used on a plan view to better identify instability across regions. EPV provides a quantitative value to assess the presence of conditional symmetric instability (CSI; Moore and Lambert 1993). CSI can result in slantwise convection and yield a substantial increase of snow totals over a narrow band. However, if vertical instability exists, the upright convection will dominate CSI and the corresponding slantwise convection. A parcel with negative EPV is convectively unstable, either vertically or slantwise (McCann 1995). If EPV is negative, θ_e decreases with height, and the atmosphere is saturated then the atmosphere is potentially unstable and supportive of upright convection. If EPV is negative, θ_e increases with height, and the atmosphere is saturated then CSI is present. If EPV is positive then the atmosphere is potentially stable (Schultz and Schumacher 1999). Even in a weakly stable region (< .25 EPV), it is still possible to have elevated convection given sufficient frontogenetical forcing in a region of weak symmetric stability (Moore and Lambert 1999).

4.3 Combination of Fgen/Instability leading to Heavy Precipitation

Through the use of EPV and frontogenesis plotted on cross sections, an explanation of the likely mechanism responsible for the precipitation will be explored. Cross sections were taken perpendicular to the 850 – 300 mb thickness values which were also perpendicular to the snow band (Fig. 11). The cross section line extended from southeastern Ellis County northwestward into northwest Montague County, but the axis of snowfall corresponds to the NW half (left side) of the cross sections. The fields in the cross section consisted of 2-D Petterssen Frontogenesis, θ_e lapse rates, and EPV. These fields were used to analyze the conditional stability of the atmosphere.

The axis of heavy snowfall was well correlated with the 700 mb frontogenesis axis between 1800 and 2100 UTC. The critical level for precipitation appeared to be 700 mb because it contained the unique combination of elevated instability, frontogenesis, and high moisture content. The 700 mb front was quasi-stationary during this period and did not move south until the 700 mb low center moved northeast of the region, which occurred by 2100 UTC. Precipitation ended with the passage of the 700 mb front due to forcing from downward vertical motions associated with cold air advection.

At 1700 UTC there was a large area of negative EPV (blue shaded) throughout most of the 600 – 700 mb layer across the cross section (Fig. 12). The white shaded regions in the cross section depict negative θ_e lapse rates. The areas of both negative lapse rates and negative EPV were regions of conditional instability (CI). The remainder of the layer from 600 to 700 mb with negative EPV values and positive θ_e lapse rates (non-white) were areas where slantwise convection was likely to occur. Therefore, the area of CI was embedded in a large area of CSI and thus, the upright convection would dominate over the slantwise convection in this region (Moore and Lambert 1993). Also overlaid in the cross section is frontogenesis. Relative humidity was omitted from these diagrams because in this event the atmosphere was nearly saturated allowing parcels to tap into the instability and CSI.

At 1800 UTC, the banding of precipitation had begun (Fig. 13) and the cross section (Fig. 14) showed a similar setup as in the 1700 UTC cross section. The frontogenesis had become stronger with a wide swath of $30 \text{ K m}^{-1} 10^{10} \text{s}^{-1}$ values below 700 mb in the southeastern two-thirds of the cross section. The negative θ_e lapse rates and corresponding instability was still ongoing on top of the frontogenesis maximum and embedded in a large area of negative EPV (CSI).

At 1900 UTC, the frontogenesis was still strong, but there was no longer an area of negative θ_e lapse rates and therefore conditional instability was no longer present in the area of the heavy snow band (Fig. 15). There still was a large region of negative values of EPV (CSI), but this region was beginning to show signs of stabilizing.

At 2000 UTC, frontogenesis remained strong, but was now beginning to shift southeast. The atmosphere in the area of interest had transitioned into a weakly symmetric stability region with EPV values less than 0.25 but remaining positive (Fig. 16). The atmosphere remained nearly saturated and heavy precipitation was still possible due to strong frontogenesis as suggested by Moore and Lambert. The 2030 UTC radar image showed the precipitation shifting to the southeast with the movement of the 700 mb front (Fig. 17).

To summarize, based on the RUC analyses, CSI was analyzed in the atmosphere, with a pocket of CI present at the beginning of the event situated above the frontogenesis maximum. This CI was exhausted

within two hours into the heavy precipitation event, but the atmosphere continued to allow the release of CSI. All precipitation came to an end with the passage of the 700 mb front.

5. Precipitation Type

The heavy snow band with this event was situated just north of the rain/snow line which made forecasting precipitation type and snowfall amounts difficult. Prior to the onset of precipitation at 1500 UTC, the temperature of the atmosphere from the surface to 800 mb was above freezing in Wise County (Fig. 18). Light precipitation began to fall around 1600 UTC, and by 1700 UTC temperatures had cooled slightly due to evaporative cooling but precipitation was still in liquid form (Fig. 19). The column did not cool entirely below 0°C until 1800 UTC when strong frontogenetic lift commenced and cooled the entire layer adiabatically (Fig. 20). In the absence of the strong frontogenetical lift, the warm air advection at 700 mb to 800 mb would have caused the temperature to remain above 0°C. This event was unique in that strong warm-moist advection helped create a favorable environment for precipitation, while the intense frontogenesis appeared to offset this warming influence to dynamically lift and cool the layer below 0°C.

6. Lightning

This event also contained several cloud-to-ground lightning strikes within the heavy snow band. Thundersnow is a very rare occurrence across the Contiguous United States with only 6% of all freezing or frozen precipitation events reporting thunder, although this number may be underrated given the scarcity of observation sites (Branick, 1997). There were five lightning strikes in the snow band between 1800 UTC and 1900 UTC observed with the National Lightning Detection Network (NLDN) as well as three area airports, which also corresponds to when CI was present. KMWL (Mineral Wells, TX) observed thundersnow at 1826 UTC, KDTO (Denton, TX) observed thundersnow at 1840 UTC, and KGVI (Sherman, TX) observed thundersnow at 1842 UTC. After 1842 UTC, additional cloud-to-ground lightning strikes were detected by the NLDN in Northeastern Wise County and Southwestern Cooke County between 1930 and 2000 UTC when only CSI was analyzed.

Another interesting data set included total lightning information from Vaisala's Lightning Detection and Ranging System II (LDAR II) from the Dallas-Fort Worth area. LDAR II detects > 95% of all total (cloud plus cloud-to-ground) lightning flashes and can map the horizontal extent of these flashes in three dimensions. Since the majority of lightning stays in the clouds and never reaches the ground, VHF lightning detection networks, such as LDAR II, can provide valuable thunderstorm data for the meteorological community (Patrick and Demetriades 2005).

At 1802 UTC, a cloud flash originated in Northwest Denton County according to the flash initiation density field from LDAR II. The flash then branched out and ended 31 km (19 miles) away in Southeast Cooke County (Fig. 21). At 1826 UTC, there were six in-cloud flashes observed around the snow band (Fig. 22). Several of these flashes spread within the cloud, but were not as long as the flash in Fig. 21.

Market et al. (2006) examined eleven cases of thundersnow and corresponding proximity upper air soundings versus cases that had similar synoptic patterns and had no thunder. They made determinations on several variables which would favor a thundersnow event versus a non thundersnow event.

A special upper air observation at 1800 UTC (see Fig. 10) from FWD was approximately 32 km (20 miles) SE of the heavy snow band. The atmosphere sampled by the balloon at 1800 UTC was just to the south of the 700 mb frontogenesis maximum and area of the maximum elevated instability. The balloon was also launched prior to the onset of the strengthening frontogenesis and heavy precipitation. Therefore, the 1800 UTC sounding was modified to adiabatically lift the column of air from 600 mb to 700 mb to approximate the effect frontogenetic lifting would have on elevated instability in order to be more representative of the atmosphere within the band of precipitation (Fig. 23). This cooled the column in the 600 mb to 700 mb slightly.

Market et al. noted that the 500 – 700 mb mean temperature lapse rates in thundersnow cases was 6.5 K km^{-1} and in non-thundersnow cases the mean lapse rate was 5.5 K km^{-1} . The amended 1800 UTC FWD RAOB had a lapse rate of 6.56 K km^{-1} . Of the eleven cases examined by Market et al., only four

cases revealed CAPE of any kind. A parcel lifted from 700 mb in the altered 1800 UTC FWD RAOB had a CAPE value of 5 J/kg with no CIN present.

One last interesting feature was a strong correlation to the observed cloud-to-ground lightning strikes and the region of negative θ_e lapse rates during the beginning of the event with the 1700 UTC 650 mb–700 mb theta-E lapse rates (Fig. 24). The instability in this layer was just at or slightly above the frontogenesis maximum and best depicted where the instability was located prior to the onset of the heavy precipitation. All cloud-to-ground lightning strikes observed by the NLDN fall into the areas of negative lapse rates or areas of instability.

7. Concluding Remarks

Heavy snowfall over North Texas is very rare and as a result is difficult for forecasters to anticipate. Forecasters must have an understanding on how the dynamics of frontogenesis, CSI, and CI can alter the atmosphere and greatly influence snowfall amounts when combined with sufficient moisture. In this event, it was shown that strong frontogenesis was present at various layers throughout North Texas, but played a critical role at 700 - 800 mb in altering and cooling the thermal profile below freezing despite strong WAA. In addition, the combination of strong frontogenetic lift and warm air advection led to elevated instability for parcels around 700 mb and contributed to intense snowfall rates and occasional lightning discharges. An analysis of the moisture and instability fields allowed us to conclude that upright convection dominated during the first half of the snowfall event before transitioning to slantwise convection as instability was exhausted.

Acknowledgements:

We would like to thank Gregory Patrick for reviewing our paper before publication and for archiving all local data of this event locally at the National Weather Service office in Fort Worth.

References:

- Benjamin, S.G., B.E. Schwartz, and R.E. Cole, 1999: Accuracy of ACARS wind and temperature observations determined by collocation. *Wea. Forecasting*, **14**, 1032-1038.
- Bergeron, T., 1928: Über die dreidimensional verknüpfende Wetteranalyse I. *Geof. Publ.*, **5**, No. 6, 1-111.
- Bluestein, H. B., 1993: *Synoptic-Dynamic Meteorology in Midlatitudes. Volume II: Observations and Theory of Weather Systems*. Oxford University Press, 594 pp.
- Branick, M. L., 1997: A Climatology of Significant Winter-Type Weather Events in the Contiguous United States, 1982-94. *Wea. Forecasting*, **12**, 193-207.
- Brusky, E. S. and R. D. Mamrosh, 2006: The Utility of Aircraft Soundings in Assessing the Near Storm Environment. *23rd Conference on Severe Local Storms*, St. Louis, MO, Amer. Meteor. Soc.
- Market, P. S., et al, 2006: Proximity Soundings of Thundersnow in the Central United States. *Journal of Geophysical Research*, **2**, D19208, 1-10.
- _____, and R. L. Ebert-Cripe, 2007: Case Study of a Long-Lived Thundersnow Event. *National Weather Digest*, **31**, No. 2, 103-119.
- McCann, D. W., 1995: Three-Dimensional Computations of Equivalent Potential Vorticity. *Wea. Forecasting*, **10**, 798-802.
- Moore, J. T., and T. E. Lambert, 1993: The use of equivalent potential vorticity to diagnose regions of conditional symmetric instability. *Wea. Forecasting*, **8**, 301-308.
- Nicosia, D. J., and R. H. Grumm, 1998: Mesoscale Band Formation in Three Major Northeastern United States Snowstorms. *Wea. Forecasting*, **14**, 346-368.
- Patrick, G. R. and N. W. S. Demetriadis, 2005: Using LDAR II total lightning data in an operational setting: experiences at WFO Fort Worth, TX. *21st Conference on Weather Analysis and Forecasting, 17th Conference on Numerical Weather Prediction*, Washington D.C., Amer. Meteor. Soc.
- Schultz, D. M., and P. N. Schumacher, 1999: The use and misuse of conditional symmetric instability. *Mon. Wea. Rev.*, **127**, 2709-2732.
- Stone, P. H., 1966: Frontogenesis by Horizontal Wind Deformation Fields. *Journal of Atmospheric Sciences*, **23**, No. 5, 455-465.

Figures

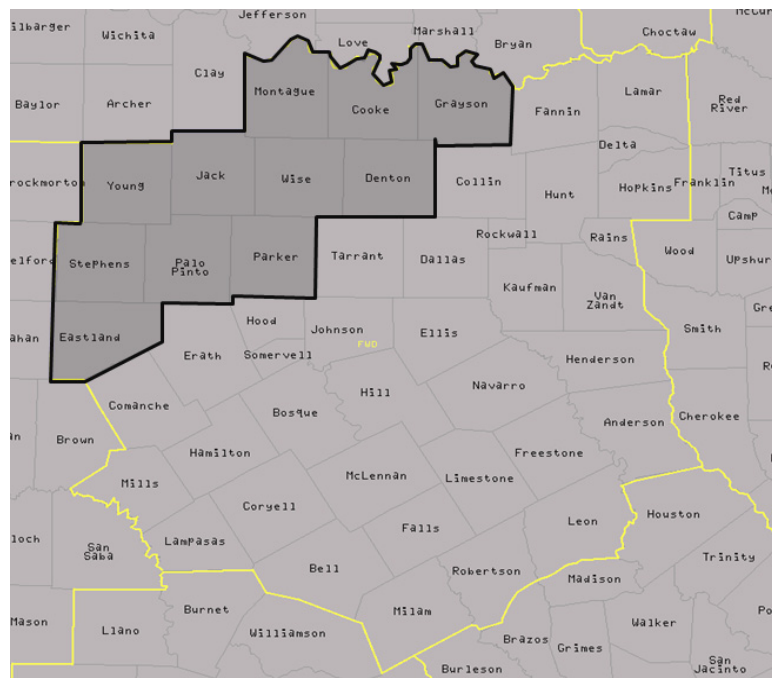


Fig. 1. A map of the National Weather Service Fort Worth County Warning Area (CWA) with the yellow lines indicating the CWA Boundaries. The darker grey shaded region with black outline is the area of interest for this study.

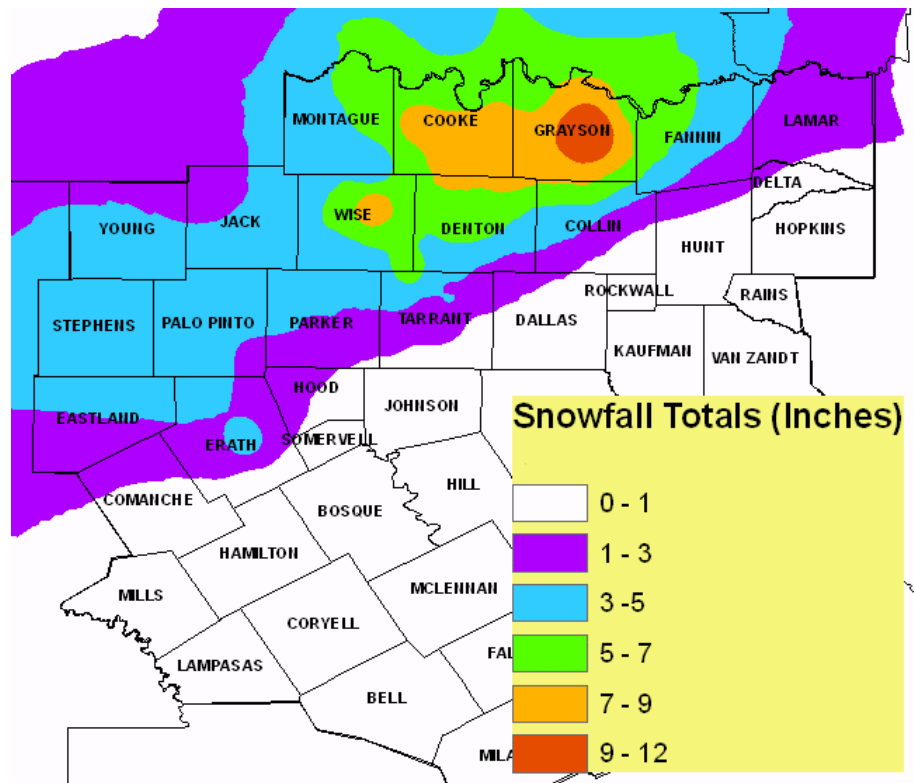


Fig. 2. Map of Snowfall totals for 6 March 2008. The greatest snowfall amounts were reported north of the Dallas/Fort Worth Metroplex across Wise, Denton, Cooke, and Grayson Counties.

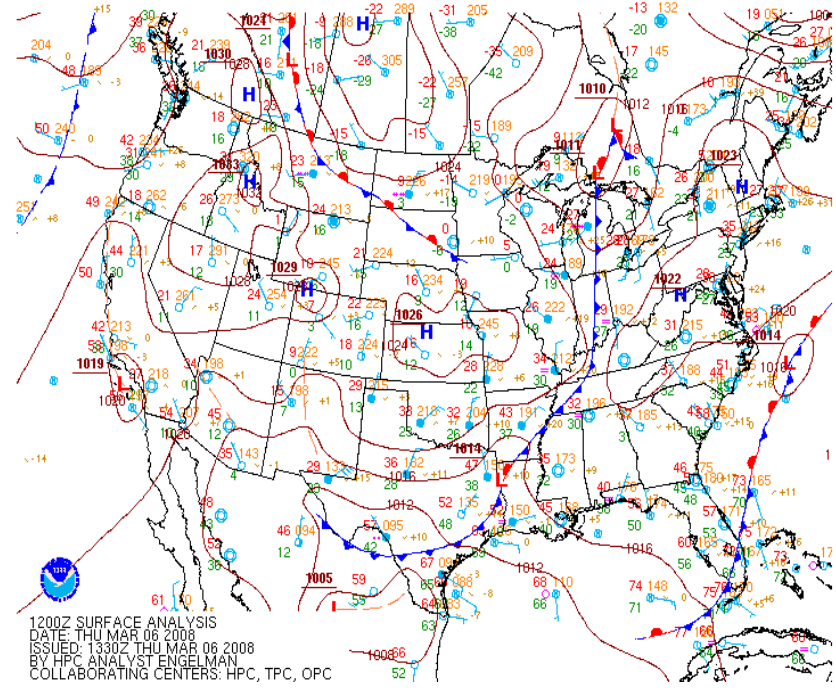


Fig. 3. 1200 UTC 6 March 2008 surface analysis from the Hydrometeorological Prediction Center (HPC). Surface cold front is depicted with a blue line which extends from Michigan into Texas. Surface METAR observations are in cyan. Isobars are depicted by the brown lines.

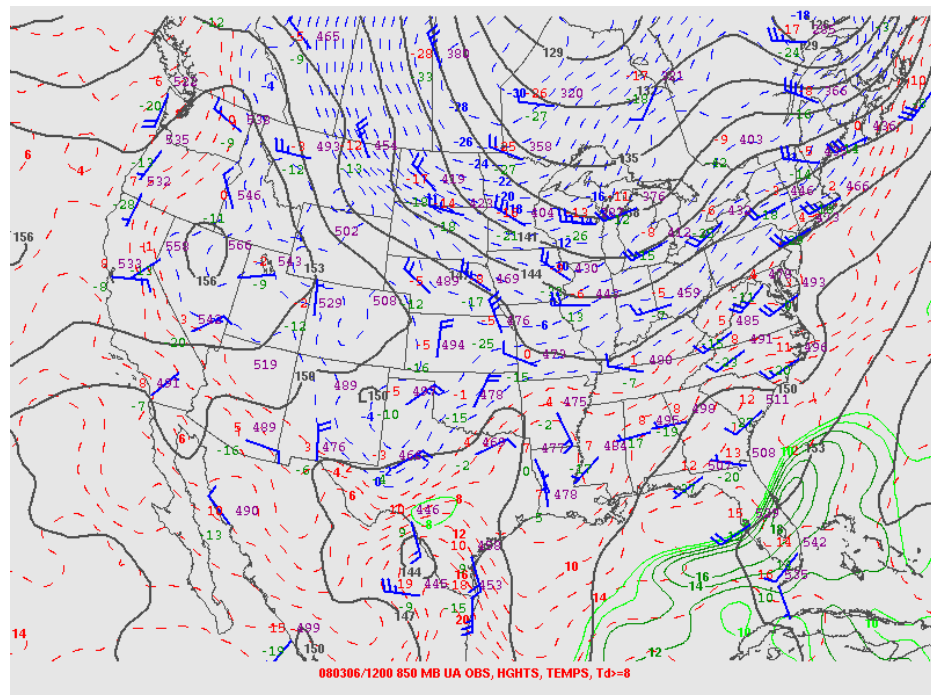


Fig. 4. Objectively analyzed 1200 UTC 6 March 2008 850 mb upper air chart from the Storm Prediction Center (SPC). Temperature contours are dotted lines, with above freezing lines shown in red and at or below freezing shown in blue. Isoheights are depicted by solid black lines. Upper air observation sites are shown by the solid blue wind barb.

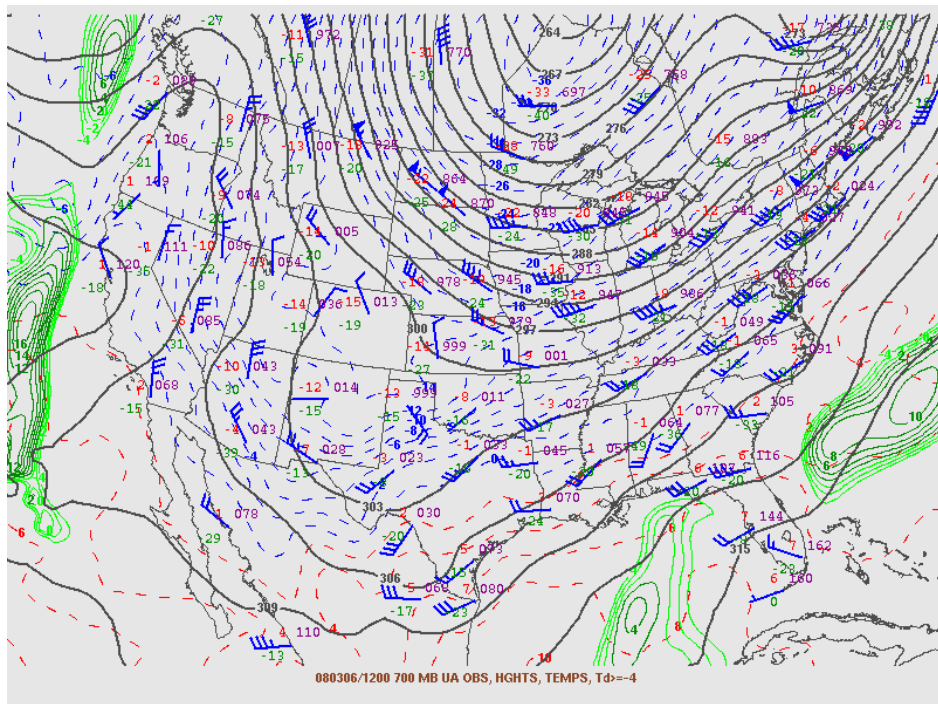


Fig. 5. Objectively analyzed 700 mb upper air chart from SPC. Fields are same as Fig. 4.

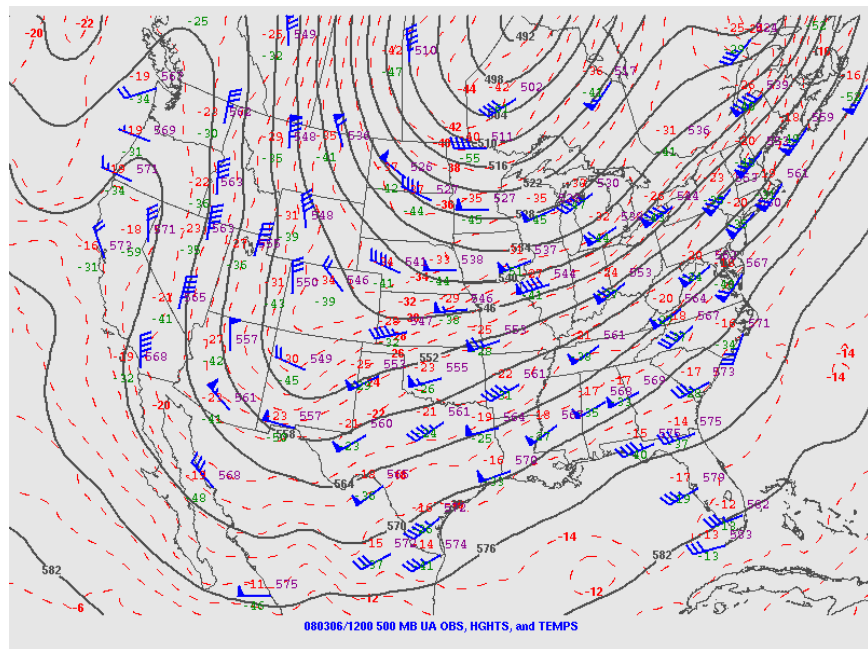


Fig. 6. Objectively analyzed 500 mb upper air chart from SPC. Fields are same as Fig. 4 except all temperature contours are shown by red dotted lines.

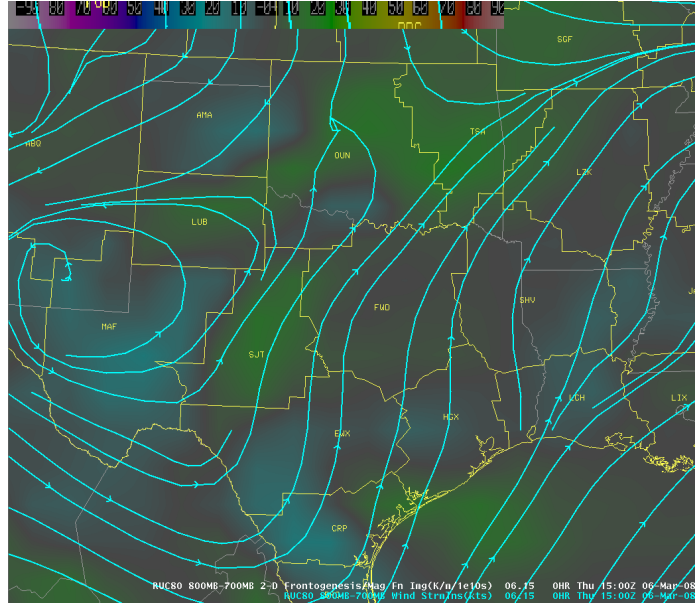


Fig. 7. 1500 UTC 800 – 700 mb wind streamlines in cyan show a cyclonic circulation centered over West Texas, a broad trough in Northeastern Oklahoma, and weak ridges over Louisiana and the Texas Panhandle. This pattern yields a deformation zone stretching from near San Angelo northeastward into Oklahoma. The background image is 800 – 700 mb frontogenesis. Green and Yellow or warm colors indicate positive values of frontogenesis and the blue or cool colors indicate negative values of frontogenesis. All fields are from the 00 hour RUC on an 80 km grid.

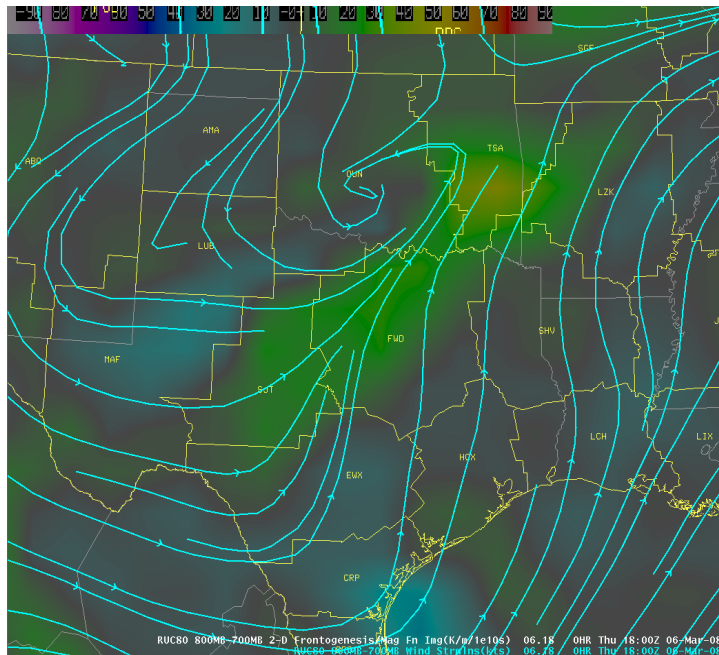


Fig. 8. Same as Fig.7, except valid time is 1800 UTC. The deformation zone aided in the tightening of the temperature gradient resulting in strengthening frontogenesis.

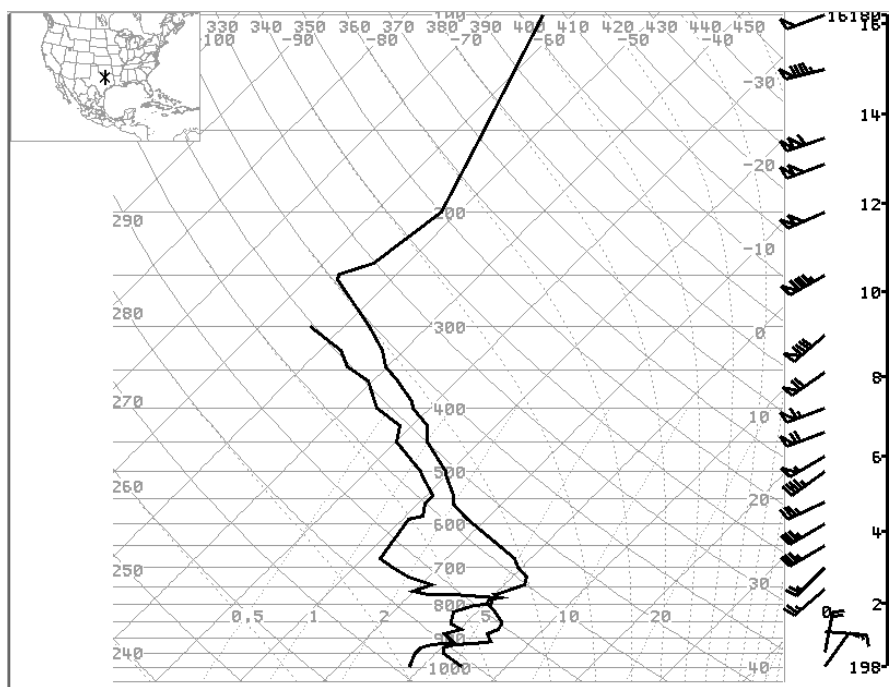


Fig. 9. The observed sounding taken from the Weather Forecast Office in Fort Worth, TX at 1200 UTC 6 March 2008. Note the stable layer extending from 925 mb to 700 mb with steep lapse rates above the inversion.

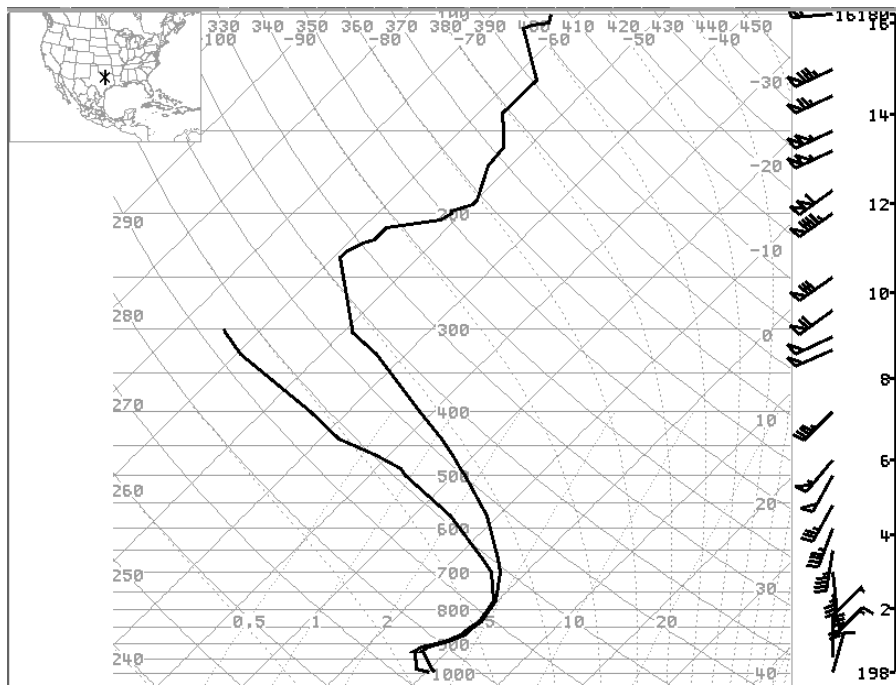


Fig. 10. The observed sounding taken from the Weather Forecast Office in Fort Worth, TX at 1800 UTC 6 March 2008. This sounding compared to the 1200 UTC sounding in Fig. 9 showed how the thermal profile in the 900 mb – 700 mb layer had cooled and moistened significantly.

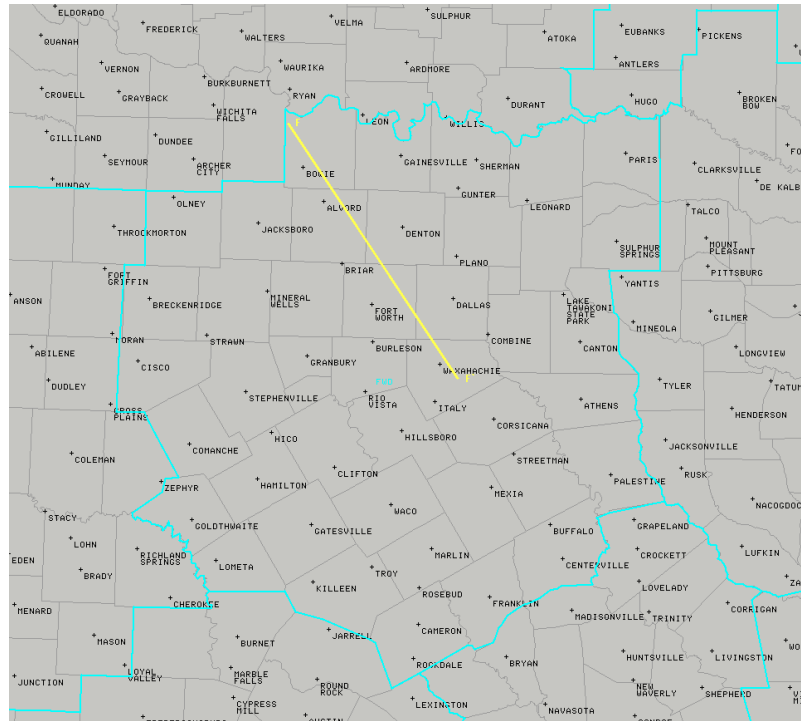


Fig. 11. The line used for the vertical cross sections in subsequent figures, extending from southeast of Waxahachie, TX in Ellis County northwestward to northwest of Bowie, TX in Montague County.

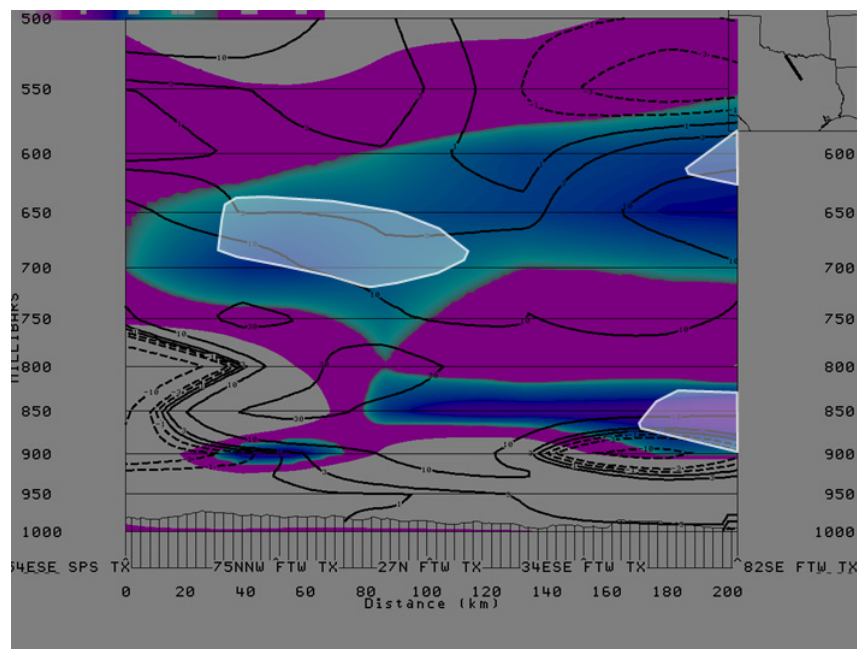


Fig. 12. Cross section taken from line shown in Fig. 11 at 1700 UTC 6 March 2008 analyzed by the RUC on a 40 km grid. Black contours are values of 2-d frontogenesis in $\text{K m}^{-1} 10^{10} \text{s}^{-1}$ with solid lines indicating positive values and dotted lines indicating negative values. The background image depicts values of EPV. Blue shades depict areas of negative EPV and pink shade represents values between 0 and 0.25 which would indicate weak stability. The white shaded regions are areas of negative θ_e lapse rates.

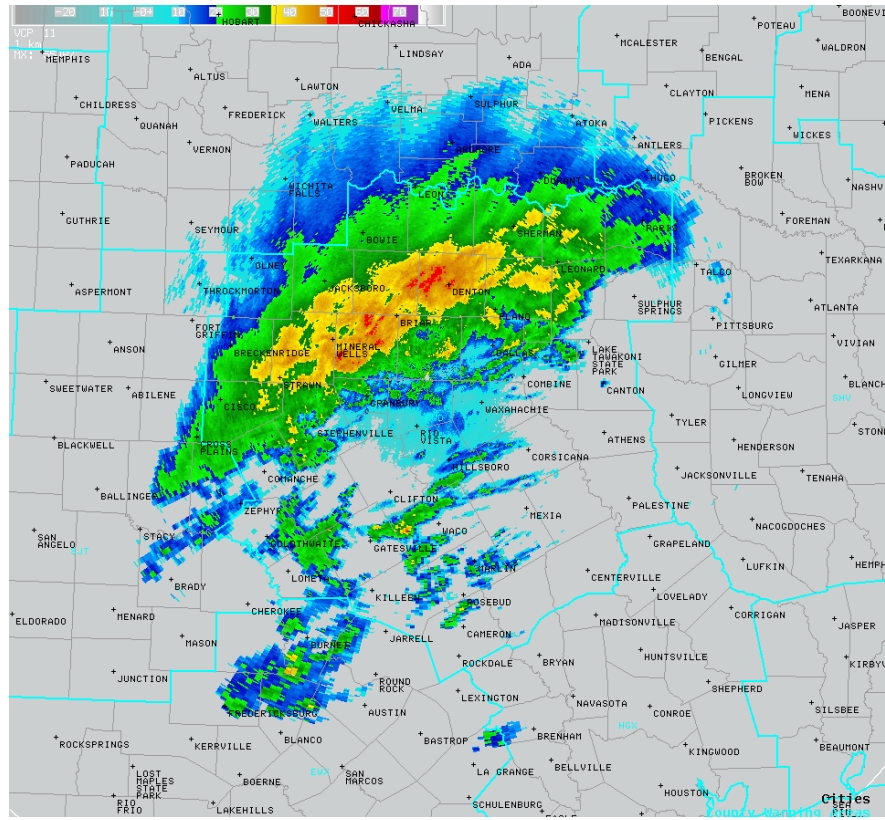


Fig. 13. 0.5 degree reflectivity image from WSR-88D at Fort Worth Spinks Airport (FWS) taken at 1800 UTC 6 March 2008.

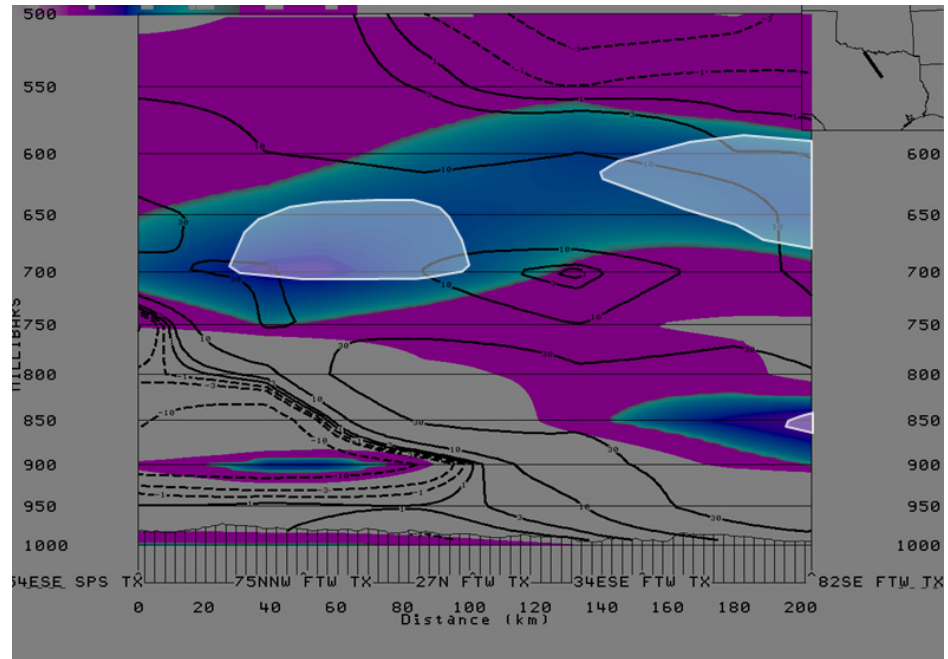


Fig. 14. Same as Fig.12 except at 1800 UTC.

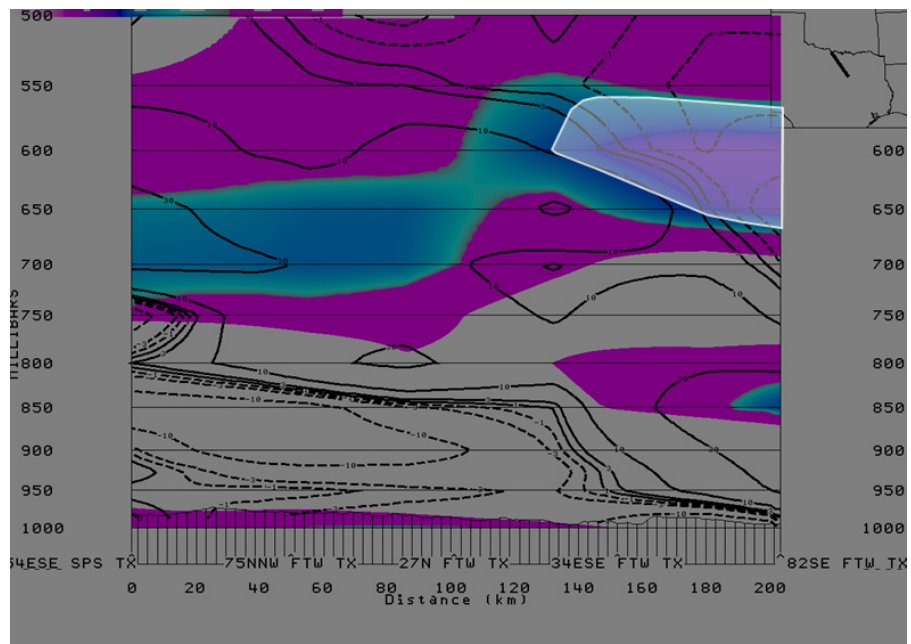


Fig. 15. Same as Fig.12 except at 1900 UTC.

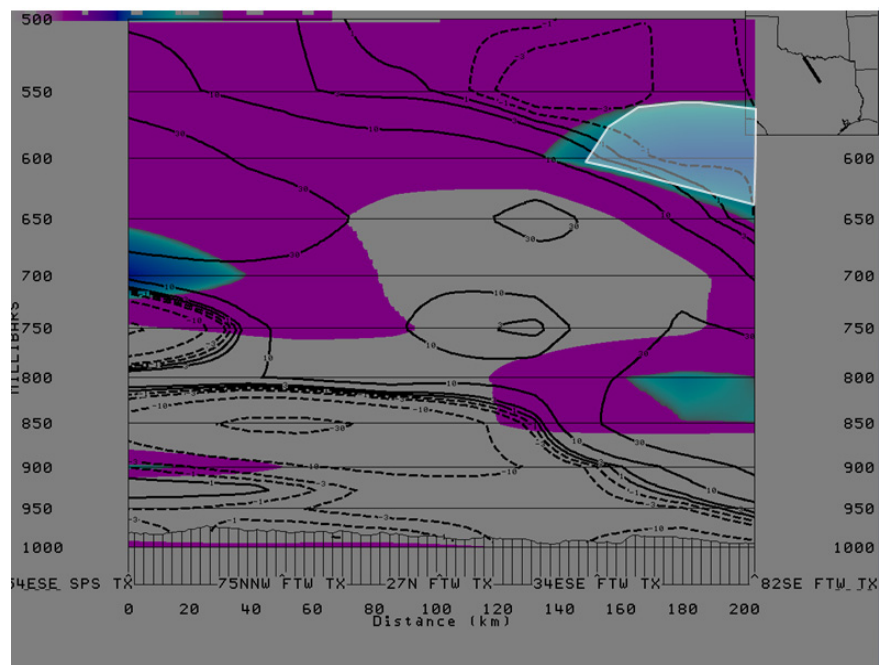


Fig. 16. Same as Fig.12 except at 2000 UTC.

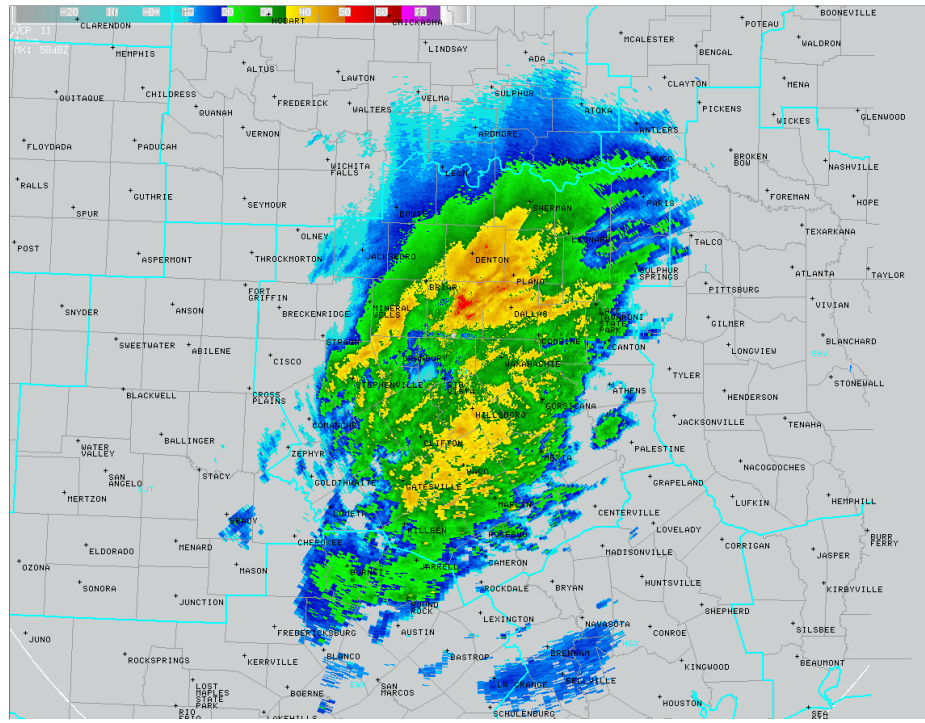


Fig. 17. Reflectivity image at 0.5 degree from KFWS at 2030 UTC 6 March 2008.

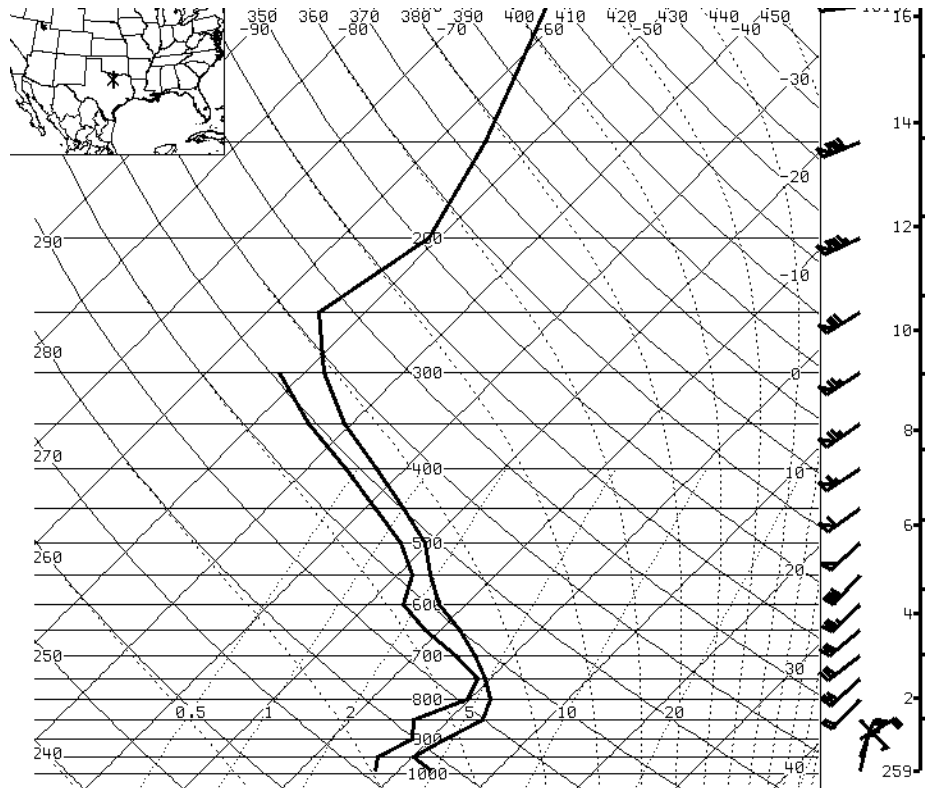


Fig. 18. 40 km RUC analysis point sounding at 1500 UTC for southeast Wise County. Temperature data is shown by the line on the right, dewpoint is shown by the left line, and wind data is shown on the right depicted by the wind barbs.

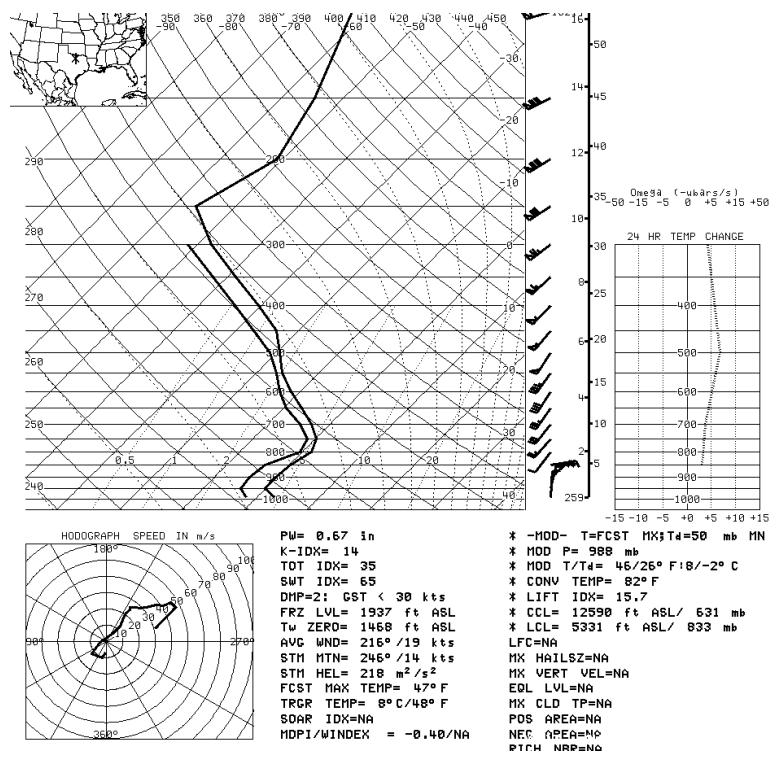


Fig. 19. 0-hour 40 km RUC Skew-T chart at 1700 UTC for a point in southeast Wise County.

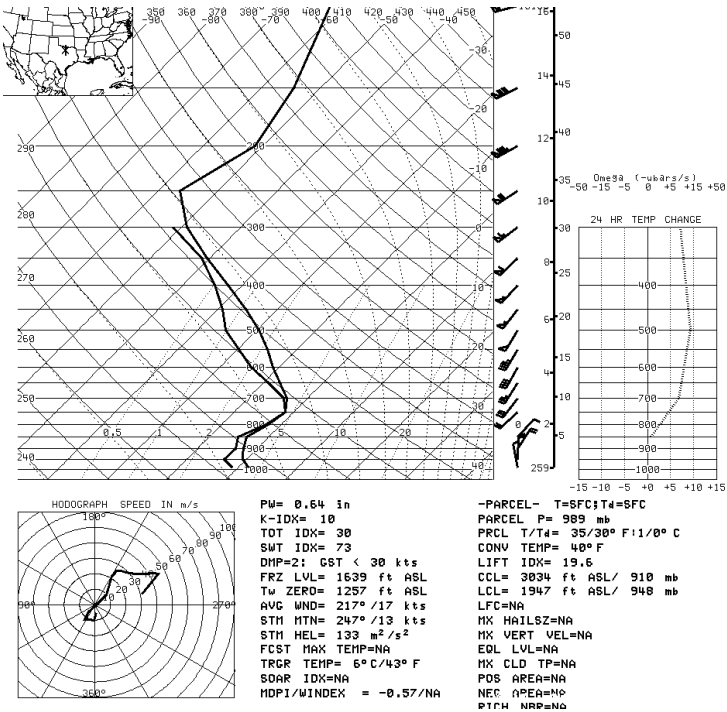


Fig. 20. 0-hour 40 km RUC Skew-T chart at 1800 UTC for a point in southeast Wise County.

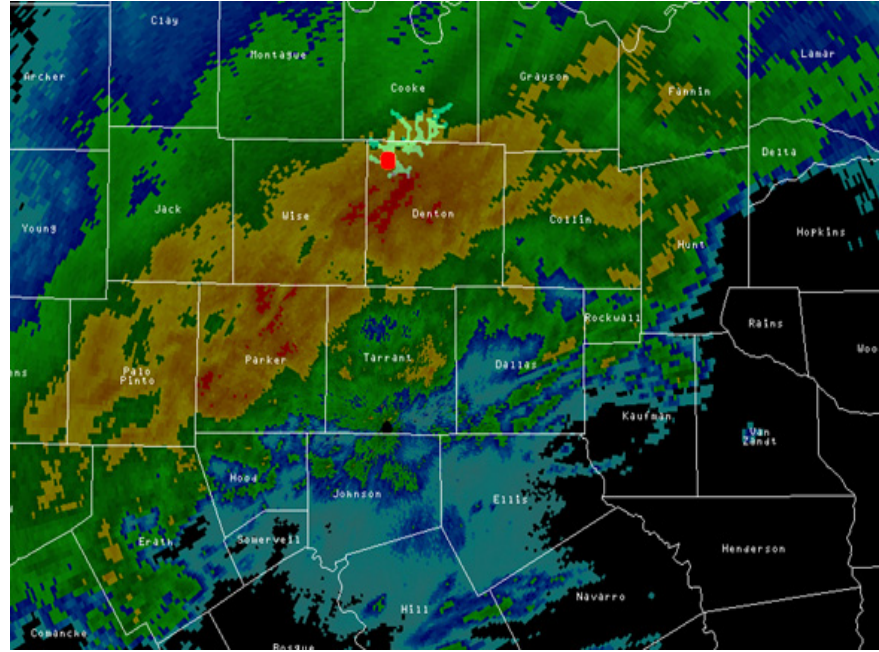


Fig. 21. 1802 UTC Radar Reflectivity from FWS is in the background, the red dot is the point of initiation of a cloud lightning flash, and the green lines are the path the lightning flash travelled in the cloud. This image is based on mapping created by LDAR II (see Demetriades and Patrick 2008).

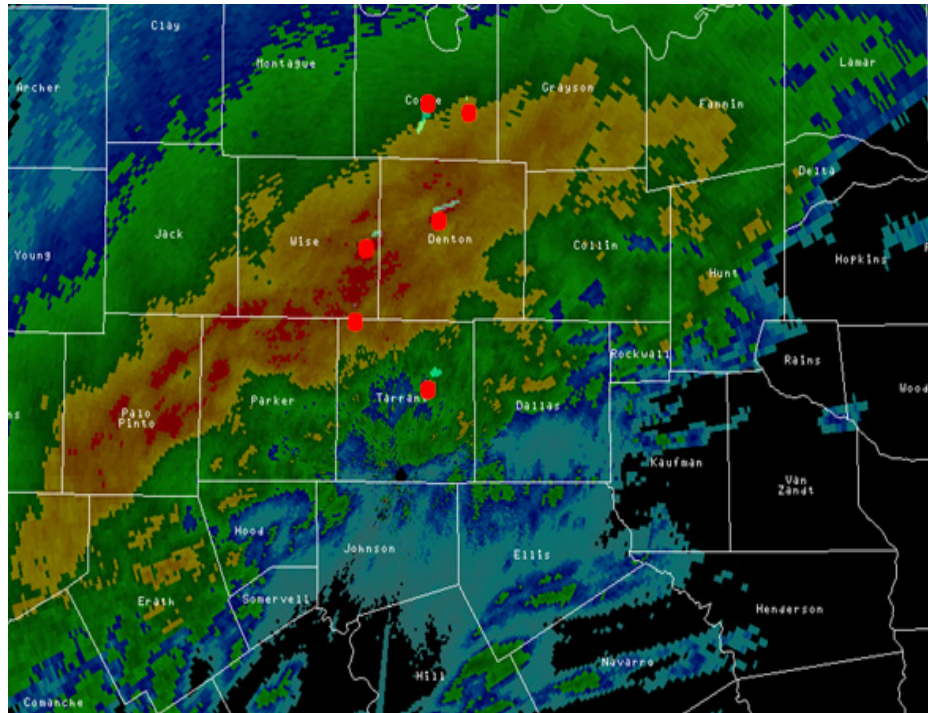


Fig. 22. 1826 UTC Radar Reflectivity from FWS is in the background, the red dots are the points of initiation, and the green lines are the path the lightning flashes travelled in the cloud.

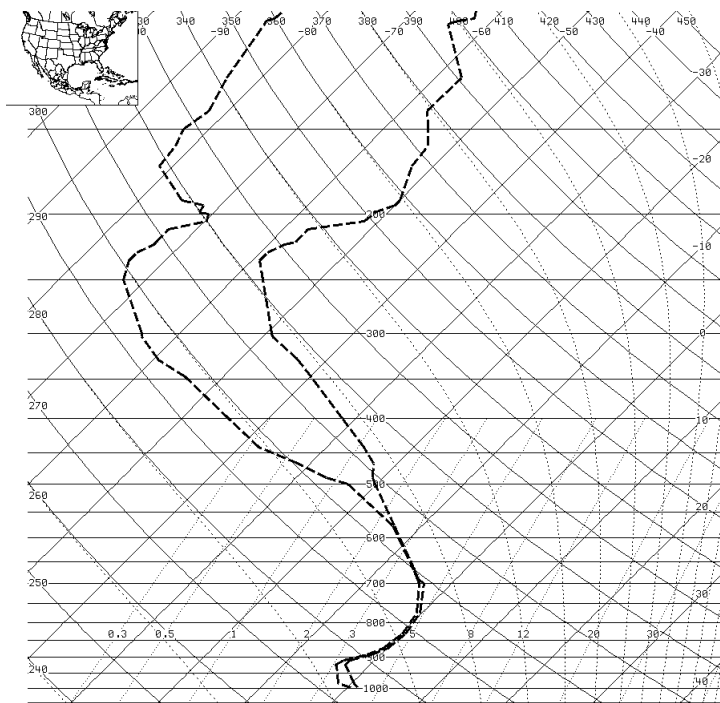


Fig. 23. Modified 1800 UTC FWD RAOB to account for adiabatic cooling from 600 mb to 700 mb. The resulting 500 mb – 700 mb lapse rate was 6.56 K km^{-1} .

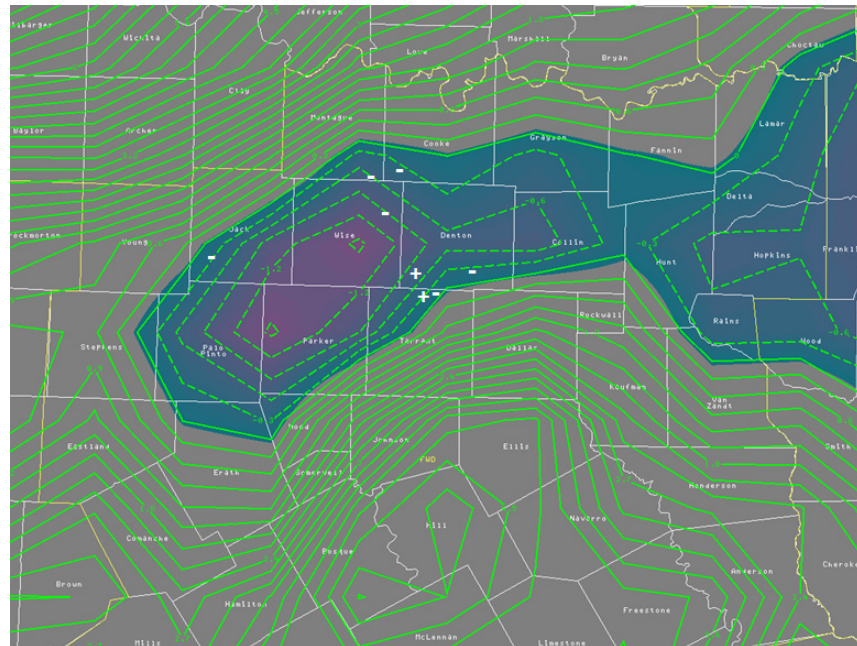


Fig. 24. Background image highlights negative values of theta-E lapse rates in the purple and blue shades. Green contours are constant values of theta-E lapse rates. Dotted contours represent negative lapse rates and solid contours are positive values. Data is from the 00 hour 1700 UTC RUC on a 40 km grid and is looking at the 650 mb to 700 mb layer. Positive and negative signs indicate locations and polarity of cloud to ground lightning strikes.